Journal of Water Sciences Research,
ISSN: 2251-7405 eISSN: 2251-7413
Vol.7, No.1, Autumn 2015, 53-61, JWSR

JWSR

Numerical Simulation of Sediment Distribution and Transmission in Pre-Sedimentation basins Using FV Method and Comparison with the Experimental Results

Mohammad Reza Borna[1*], Mohammad Reza Pirestani[2]

1. Ph.D. Candidate, Department of Civil Engineering, Central Tehran branch, Islamic Azad University, Tehran, Iran

2. Assistant Professor, Department of Civil Engineering, South Tehran branch, Islamic Azad University, Tehran, Iran

Received: 15 December 2015 Accepted: 12 March 2015

ABSTRACT

Pre-sedimentation basins are among the most important elements of the conventional water treatment process. In pre-sedimentation basins, due to different velocity gradients, secondary and rotational flows are formed that will create short paths and increase dead and still flow zones as well as changes in the flow mixing. This will prevent laminar flow conditions for sedimentation and will reduce the basin efficiency. The first step in optimization of the pre-sedimentation basins is the correct calculation of the velocity field and rotating zones volume. In this study, flow in a rectangular basin was simulated numerically and continuity and Novier-Stokes equations were solved using the Finite Volume method. 3-D flow simulation was performed using standard k-ε turbulence model and flow velocity profiles at different sections of the pre-sedimentation basin were compared with the experimental results and the results were in good agreement. Then, in order to investigate the sedimentation pattern in pre-sedimentation basin, convection-diffusion equation of the sediment concentration was simultaneously solved with the governing equations of the flow hydraulics. Finally, vertical distribution of sediment concentration at different basin sections was compared with the experimental and numerical results of other researchers. The results indicated a good agreement between the numerical and experimental results as well as the model ability to predict sediment distribution profiles in pre-sedimentation basins.

Keywords

Pre-sedimentation Basins, Flow Velocity Profile, Sediment Concentration and Distribution

1. Introduction

Given the importance of drinking water quality and high efficiency of the water treatment process, performance of the pre-sedimentation basins is considered. Pre-sedimentation basins separate flow particles so that in water treatment plants, coagulants are added to the flow before pre-sedimentation basin in quick mixing basin to increase particles size and decrease the sedimentation time. Heavy sediment particles settle on the basin floor as sludge. Due to high construction and maintenance cost of the basins, optimum performance of the basins is of utmost importance. Despite the importance of the basins, the existing designs rely heavily on the simple experimental formula and hydrodynamics of the system are neglected. Performance of the pre-sedimentation basins are highly influenced by the hydraulic and physical effects such as flow density, gravity and sediment coagulation. In this regard, the chemical aspect of the sediment in the basin is not the only important one, but flow hydraulics plays an important role as well. In order to optimize the basin performance, a flow with minimum

* Corresponding Author email: (mrezaborna@gmail.com)

turbulence should slowly enter the basin. The existing secondary flows and rotational regions in the basins will develop short paths and dead zones that will disturb the flow and prevent a suitable sedimentation. Therefore, the performance of the sedimentation basin is reduced. Various researchers have studied the pre-sedimentation basins experimentally and numerically. Dobbins (1994) performed an analytical and experimental study to investigate the sedimentation of the independent uniform particles in a fully-developed turbulent flow. He explained the fully developed turbulence of the flow as a condition in which despite a continue velocity is observed for each point, but the key statistic characteristics remain constant. Shiba et al. (1975) developed a method to estimate the dynamic model parameters using laboratory tests. Larsen (1977) started the initial experimental studies and used the results to develop a suitable mathematical model for the hydraulics of pre-sedimentation basins. Imam et al. (1983) performed experimental studied on a simple sedimentation basin without any flow barriers. Rodi (1984) developed a comprehensive model to estimate the flow and used transmission equation in kinetic energy. Mc. Corquodale et al. (1988) performed studies using Doppler laser. The developed model considered the basin hydrodynamics and sediment movement and sedimentation time, therefore it was considered as a reference in design of different hydraulic structures by many researchers. Lyn and Rodi (1990) studied the primary sedimentation basin of Carlsruhe by considering the inlet section. Results included vertical and horizontal velocity profiles and turbulence profiles. The study was performed by installation of a baffle in inlet. Ueberal and Hager (1997) measured velocity and concentration profiles in four sedimentation basins simultaneously from which one was as a reference and changes were applied to three other basins at different stages and results were compared. Measurements were performed for different shapes and inlet and outlet locations considering different input velocities and concentrations. Jayanti et al. (2004) simulated the hydrodynamics of the settled particles in pre-sedimentation basins and compared them with the experimental results. Findings showed that flow field could be calculated by using CFD. Tamayol and FirozAbadi (2004) simulated basins by using Fluent software and results of turbulence k-ε and RNG.

Naser et al. (2005) developed a 2D numerical and uniform model to study the hydrodynamics of the rectangular sedimentation basins in turbulence situation. In order to formulate the flow equation, integration method was used. Goula et al. (2007) simulated standard and baffled basins to investigate the flow using Fluent software. Stamou (2008) simulated a basin in Athens. He used baffles to modify the basin geometry and to increase the efficiency and decrease short paths and rotational flows. Liu et al. (2008) used modified k-ε model to evaluate turbulent flow in pre-sedimentation basins based on Boussinesq assumptions and solving the governing equations using HFAM method to simulate the pre-sedimentation basins. The present study consists of the flow hydraulics and sediments in a rectangular pre-sedimentation basin. Modelling was carried out according to Shahrokhi et al. (2011) investigations and velocity and sediment distribution profiles were compared in 3D state.

2. Materials and methods

2.1 Governing Equations

In this study, continuity and Navier-Stokes equations were solved using Finite-Volume Method that is based on the direct discretization of the conservation law in physical space. Flow was analyzed in steady state and the SIMPLE

algorithm was used for velocity and pressure coupling. Continuity, momentum, energy loss, turbulent kinetic energy and Reynolds stress equations were discretized using the second order forward method and pressure equation was discretized using the standard method.

According to the differential form of the conservation law, $\frac{\partial U}{\partial t}+\vec{\nabla}\cdot\vec{F}=Q$, the most important step in the Finite volume method is integration of the equations governing volume control the:

$$\int_{\Omega_J}\frac{\partial U}{\partial t}d\Omega+\int_{\Omega_J}\vec{\nabla}\cdot\vec{F}d\Omega=\int_{\Omega_J}Qd\Omega \quad (1)$$

According to the divergence theorem of Gauss:

$$\int_{\Omega_J}\vec{\nabla}\cdot\vec{F}d\Omega=\int_{S}\vec{F}\cdot d\vec{S} \quad (2)$$

The integral form of the conservation law for each control volume Ω_J is:

$$\frac{\partial}{\partial t}\int_{\Omega_J}Ud\Omega+\int_{S_J}\vec{F}\cdot d\vec{S}=\int_{\Omega_J}Qd\Omega \quad (3)$$

The above equation is replaced by its discrete form in which the volume integral is expressed as the averaged values in the cell and area integral as the total of the desired volume:

$$\frac{\partial}{\partial t}\left(U_J\Omega_J\right)+\sum_{faces}\vec{F}\cdot\Delta\vec{S}=Q_J\Omega_J \quad (4)$$

The governing equations on flow include continuity and momentum equations for turbulent flow and compressible flow in a 3D geometry as Eqs. (5) and (6). Turbulent kinetic energy of different turbulence models are defined as (Oslen, 2009):

$$\frac{\partial\overline{U_i}}{\partial x_i}=0 \quad (5)$$

$$\frac{\partial\overline{U}_i}{\partial t}+(\overline{U}_j)\frac{\partial\overline{U_i}}{\partial x_j}=-\frac{1}{\rho}\frac{\partial\overline{p}}{\partial x_i}+g_{xi}+\frac{\partial}{\partial x_j}[\nu\frac{\partial\overline{U}_i}{\partial x_j}-\overline{U_i'U_j'}] \quad (6)$$

$$K=\frac{1}{2}\overline{U_iU}_i \quad (7)$$

where $\rho\bar{u}_i\bar{u}_j$ is Reynolds stress, U_i and U_j are flow velocities in x and y directions, respectively, t is time, ע is molecular viscosity, p is pressure, k is turbulent kinetic energy, ρ is fluid density and g_{xi} is gravitational acceleration in xi direction. The k-ε turbulence model is used in this study in which the turbulence kinetic energy (k) is defined as follows:

$$\frac{\partial k}{\partial t}+U_j\frac{\partial k}{\partial x_i}=\frac{\partial}{\partial x_j}(\frac{V_T\partial k}{\sigma k\partial x_j})+p_k-\varepsilon \quad (8)$$

P_k is defined as:

$$P_k=\nu_T\frac{\partial U_j}{\partial x_i}(\frac{\partial U_j}{\partial x_i}+\frac{\partial U_i}{\partial x_j}) \quad (9)$$

$$\nu_T=c_\mu\frac{K}{\varepsilon^2} \quad (10)$$

$$\frac{\partial\varepsilon}{\partial t}+U_j\frac{\partial\varepsilon}{\partial x_j}=\frac{\partial}{\partial x_j}(\frac{\nu_T\partial\varepsilon}{\sigma_k\partial x_j})+C_{\varepsilon1}\frac{\varepsilon}{k}P_k+C_{\varepsilon2}\frac{\varepsilon^2}{k} \quad (11)$$

In Eq. (11), P_k is turbulence production term, and the experimental constants are as follows (Olsen, 2009).

$$C_\mu=0.09,\ C_{1\varepsilon}=1.43,\ C_{2\varepsilon}=1.92,\ \sigma_\varepsilon=1.3,\ \sigma_k=1 \quad (12)$$

In this numerical model, sediments are classified into suspended sediments and bed load. The suspended load is calculated using convection-diffusion equation as follows:

$$\frac{\partial c}{\partial t}+Uj\frac{\partial c}{\partial Xi}+\omega\frac{\partial c}{\partial z}=\frac{\partial c}{\partial Xj}(\Gamma\frac{\partial c}{\partial Xj}) \quad (13)$$

Where c is sediments concentration, ω is sediment fall velocity, U is flow velocity, X is distance and Γ is diffusion coefficient. Van Rijn (1987) developed an equation for the equilibrium concentration of sediments in the vicinity of bed (Van Rijn, 1987).

$$c_{bed}=0.015\frac{d^{0.3}}{a}\frac{\left[\frac{\tau-\tau_C}{\tau_C}\right]^{1.5}}{\left[\frac{(\rho_S-\rho_W)g}{\rho_W\nu^2}\right]^{0.1}} \quad (14)$$

Where d is the diameter of sediment particles, a is reference level of roughness

height, τ is bed shear stress, τ_c is critical shear stress, ρ_w and ρ_s are water and sediment density, respectively and ν is water viscosity.

The equation calculates sediment concentration for the cell attached to the bed. For time-dependent calculations, an algorithm that converts sediment concentration into sedimentation rate can be used. Reduced critical shear stress of sediments based on the bed slope was presented by Brooks (1963) by the following equation in which K coefficient is calculated and multiplied by the critical shear stress:

$$k = -\frac{\sin\phi\sin\alpha}{\tan\theta} + \sqrt{(\frac{\sin\phi\sin\alpha}{\tan\theta}) - \cos^2\phi[1-(\frac{\tan\phi}{\tan\theta})^2]} \quad (15)$$

where α is the angle between the flow direction and the line perpendicular to the bed, $\emptyset$ is the slope angle and θ is the slope parameter.

Van Rijn (1987) equation is used to calculate bed load (q_b):

$$\frac{q_b}{D_{50}^{1.5}\sqrt{\frac{(\rho-\rho)g}{\rho}}} = 0.053\frac{\left[\frac{t-t_c}{t_c}\right]^{1.5}}{D_{50}^{0.3}\left[\frac{(\rho-\rho)g}{\rho v^2}\right]^{0.1}} \quad (16)$$

Bed thickness form is calculated by using the Van Rijn equation (Van Rijn, 1987).

$$\frac{\Delta}{d} = 0.11(\frac{D_{50}}{d})^{0.3}\left(1-e^{\left[\frac{t-t_c}{2t_c}\right]}\right)\left(25-\left[\frac{t-t_c}{t_c}\right]\right) \quad (17)$$

Effective roughness is calculated by using the following equation:

$$k_S = 3D_{90} + 1.1\Delta\left(1-e^{\frac{25\Delta}{\lambda}}\right) \quad (18)$$

In the above equations d is water depth, Δ is bed thickness form, K_s is effective roughness and λ is length of bed form (Olsen, 2009).

3. Results and discussion

3.1 Experimental model

In the experimental study by Shahrokhi et al. (2011) a rectangular basin with the length (L) of 2 m, a width (W) of 0.5 m and a water depth to basin length ratio (H/L) of 0.155 was used. Height of the input flow to the basin (H_{in}) was 10 cm and outlet weir height (H_w) was 30 cm. Input discharge to the basin (Q) was 0.002 m^3/s, flow depth (H) was 0.31 m, input Reynolds number (Re) was 3972, sediment particle density (ρ_s) was 1.049 g/cm^3, diameter of half of sediments (d) was between 75-106 µm and another half was between 106-150 µm, experiment time (t) was 15 min , input sediment concentration (c_0) was 100 mg/l and input Froude number (Fr) was 0.04. Schematic view of the rectangular basin is shown in Fig. 1 (Shahrokhi et al., 2011).

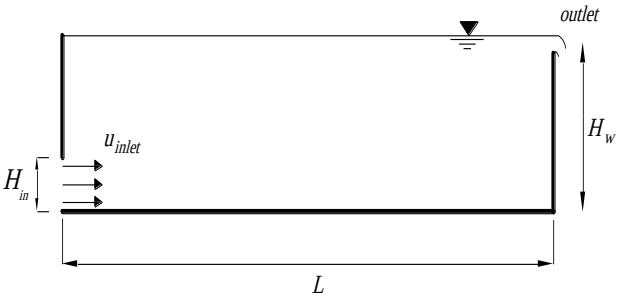

Fig. 1. Geometric characteristics of the experimental flume

3.2 Meshing and boundary conditions

In this study, an average velocity of 0.04 m/s was considered in basin inlet and output flow conditions were used in outlet boundaries. Due to small changes in water surface level, the symmetry boundary condition was applied to the water surface. The wall boundary condition was applied to the rigid boundaries and walls were considered smooth hydraulically. One of the important parameters in the running speed of the model is the appropriate meshing of the basin. Figure 2a shows the plan and 3D view of the rectangular basin meshing. The number and

size of cells in different parts in *x*, *y* and *z* directions are listed in Table 1.

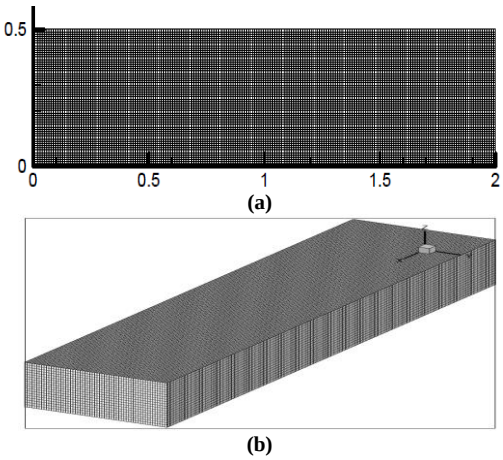

Fig. 2. Mesh of the pre-sedimentation basin in (a) Plan, (b) 3D view

Table 1. Number and size of the grid cells in the computational areas in different directions

Region	Cell dimensionsx	Cell dimensionsy	Cell dimensionsz	Cell dimensionsx (mm)	Cell (mm)dimensionsy	Cell dimension (mm)s z
Zone	250	60	19	8	8.33	16.31

3.3 Numerical simulation of the flow velocity

Figure 3 shows the non-dimensional velocity profiles (U_x/U_0) at different non-dimensional depths of the basin (z/H) for different sections (x/L) of 0.05, 0.23, 0.41, 0.59, 0.75 and 0.95 for a constant flow discharge of 0.002 m^3/s and an input Froude number (F_r) of 0.04. x and z show the distances along *x* and *z* directions of the basin, and U_0 is the input flow velocity with a value of 0.04 m/s.

As can be seen in Fig. 3, a uniform velocity profile is observed at the beginning of the basin and by getting close to the end of the basin, the maximum velocity is transferred to the bottom of the basin by moving from section x/l=0.05 to x/l=0.75. In addition, by comparing the numerical results with the experimental ones, errors occur near the bed especially in areas near the basin inlet that can be attributed to the differences in flow patterns in the inlet section. Table 2 shows the average errors at different basin sections.

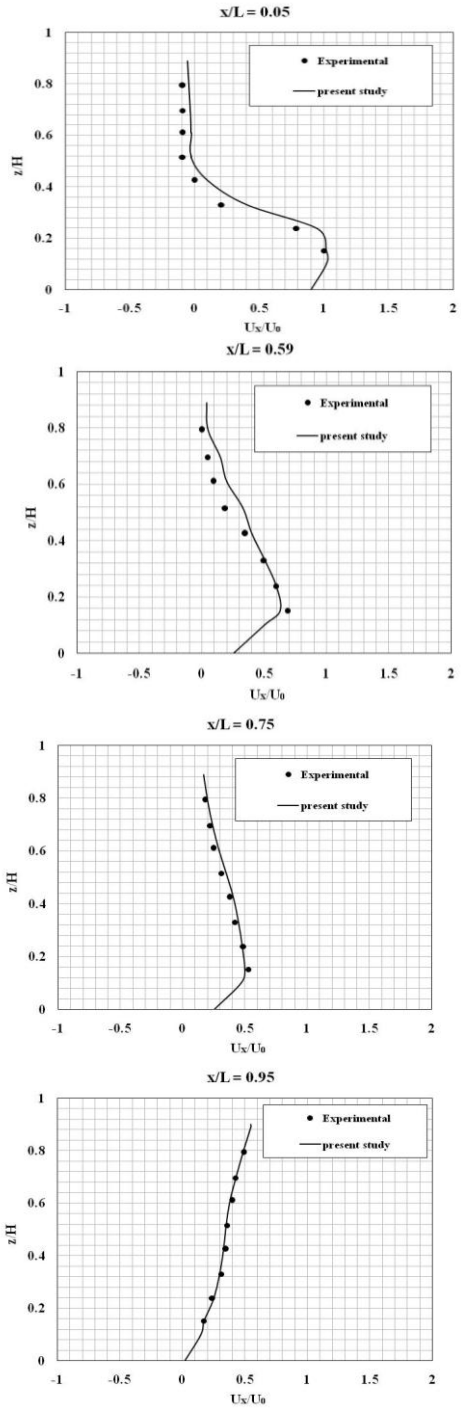

Fig. 3. Comparison of the simulated velocities at different sections of the pre-sedimentation basin with the experimental results

Table 2. Average velocity errors at different sections of the basin

Section	x/L					
	0.05	0.23	0.41	0.59	0.75	0.95
Average error in the present study	9.58	9.12	8.18	8.03	2.92	1.25

Average error percent of the velocity profiles at different sections of the basin using the numerical model shows the fairly good agreement between the numerical and experimental results. Because of the inlet location in the lower one third height of the basin, a large rotational zone is created above the basin inlet. Figure 4a shows the numerical results of the flow lines by Shahrokhi et al. (2011). In addition, Fig. 4b shows the flow lines of the present numerical model indicating a compliance with the experimental results. Shahrokhi et al. (2011) obtained a rotational flow zone with a length and width of 1.52 and 0.020 m, respectively. However, in the present study such zone with a length and width of 1.231 and 0.215 m, respectively was obtained above the basin inlet indicating average errors of 1.52 and 6.97%, respectively.

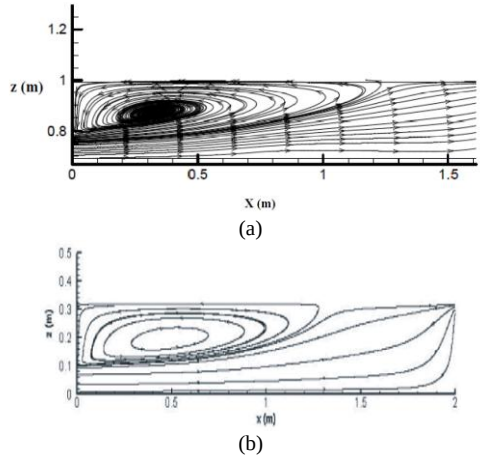

Fig. 4. Flow lines in pre-sedimentation basin in (a) the present study, and (b) Shahrokhi et al. (2011)

3.4 Numerical Simulation of sediment transmission

According to the experimental study, the vertical distribution of the sediment concentration was obtained using the numerical model at different depths (z) of the basin at different sections (x) of 84, 121, 158 and 195 cm from the basin inlet for a constant input discharge of 0.002 c/m^3, input Froude number of 0.04 and input sediment concentration (c_{in}) of 100 mg/l. Figure 5 shows the obtained results.

According to sediment distribution results shown in Fig. 5, by getting close to end of the basin, sediment concentration of the section gets close to the input concentration at levels near the bed. Figures 5 and 6 show sediment concentration profiles (c) at different basin depths (z) for different sections (x) of 84, 121, 158 and 195 cm from the basin inlet for a constant flow discharge of 0.002 m^3/s and an input sediment concentration of 100 mg/L. Numerical results were obtained from Shahrokhi et al. (2011) in which Flow 3D software was used to investigate the distribution of sediment concentration.

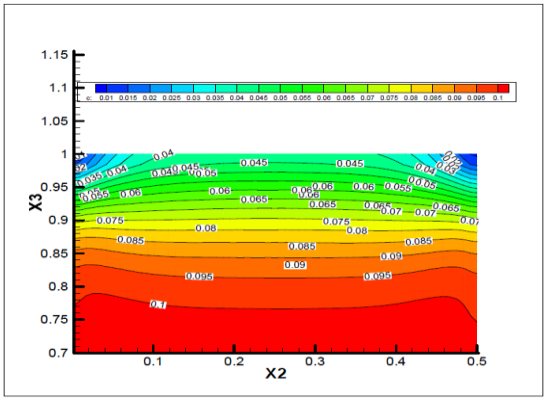

X=84 cm

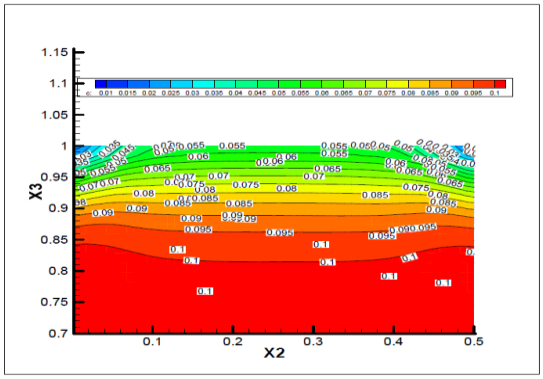

X=121 cm

Fig. 5. Graphical Evaluation of the vertical distribution of sediment concentration at different sections

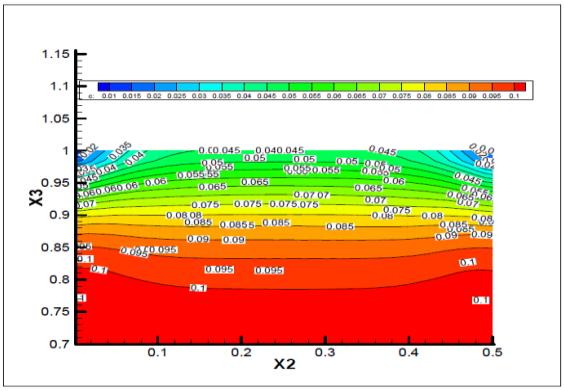

X=158 cm

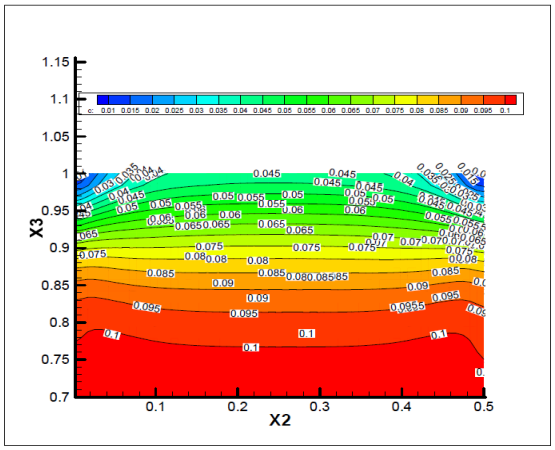

X=195 cm

Fig. 5. Continued.

According to Fig. 6, sediment concentration is increased by the depth so that in x=1.58 m, sediment concentration is 44 mg/l near the water surface that decreased about 57.48% in comparison to the bed sediment concentration.

Table 3 shows the average error of the present study comparing the numerical results obtained using Flow 3D software and the experimental results at different sections of the pre-sedimentation basin (Shahrokhi et al., 2011).

Table 3. Average error percent of the simulated results of the sediment concentration in comparison to the experimental results

Section	(X) meter			
	0.84	1.21	1.58	1.95
Current study	12.41	6.03	10.93	17.78
Simulation using Flow 3D (Shahrokhi et al. (2011)	26.54	24.25	22.43	25.96

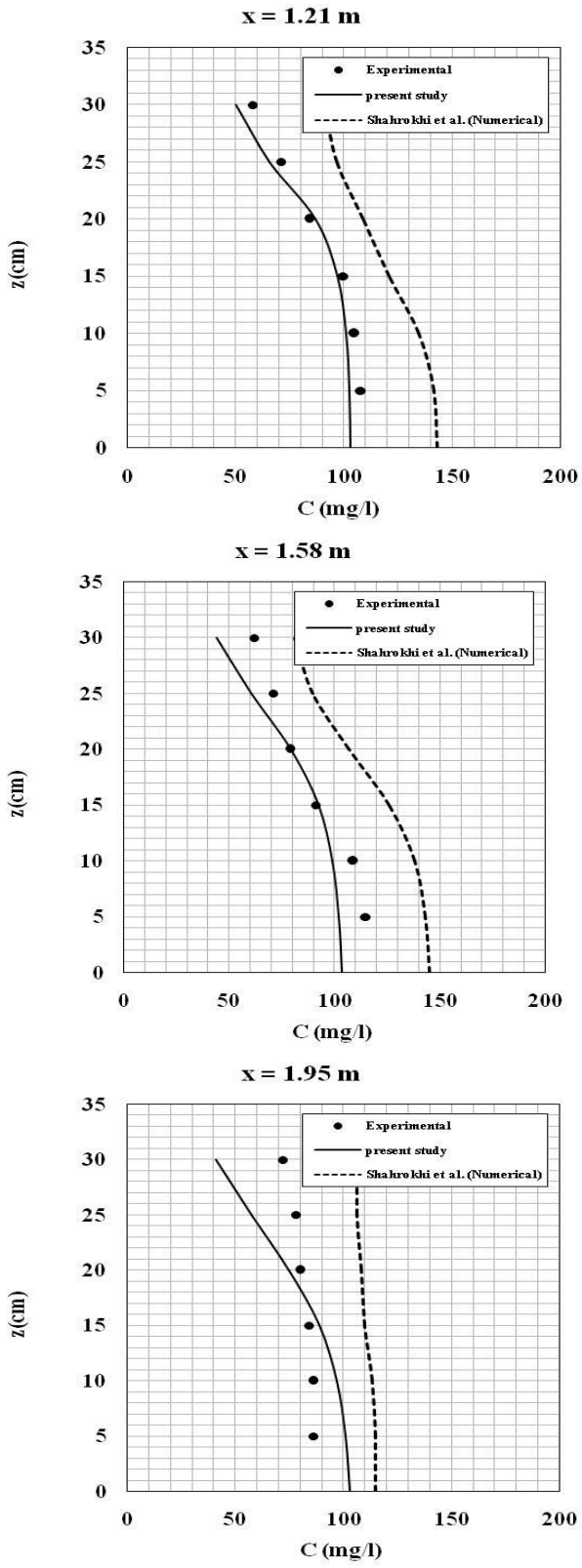

Fig. 6. Distribution of sediment concentration in different sections of the pre-sedimentation basin

According to Table 3, average errors show the good agreement between the numerical results and the experimental results.

4. Conclusions

In pre-sedimentation basins, secondary and rotational flows are formed due to velocity gradients. This will cause short paths and increase dead and still flow zones as well as changes in the flow mixing. This will prevent laminar flow conditions for sedimentation and reduce the basin efficiency. First step in optimization of the pre-sedimentation basins is the correct calculation of the velocity field. Because of the flow complexity and scale effects, physical models cannot lonely provide a clear understanding of the problem physics and the numerical simulation of the problem is needed along with the experimental and filed studies. In this study, flow hydraulics and sediment transfer and distribution in a rectangular basin is numerically simulated using the Finite Volume method. Flow was analysed in steady state and the SIMPLE algorithm was used for velocity and pressure coupling. Continuity, momentum, energy loss, turbulent kinetic energy and Reynolds stress equations were discretized using the second order forward method and pressure equation was discretized using the standard method. First, in order to study flow hydraulics in pre-sedimentation basins, the non-dimensional velocity profiles at different depths of the basin for different sections were evaluated using the standard k-ε turbulence model. Numerical results of the present study were compared with the experimental results by Shahrokhi et al. (2011) and a good agreement was observed. A uniform velocity profile was observed at the beginning part of the basin and by getting close to the end of the basin, the maximum velocity transferred to the bottom of the basin by moving from section x/l=0.05 to x/l=0.75. In addition, by comparing the numerical results with the experimental ones, errors occurred near the bed, especially in areas near the basin inlet that can be attributed to the differences in flow patterns in the inlet section. Because of the inlet location in the lower one-third height of the basin, a large rotational zone created above the basin inlet whose length and width showed average errors of 1.52 and 6.97%, respectively in comparison to the observed rotational zone in the experimental study. In order to study the flow pattern and transfer and distribution of sediments in pre-sedimentation basins, sediment distribution profiles at different depths of the basin were studied at various basin sections and the results were compared with the experimental and numerical results by other researchers. Sediment concentration decreased significantly decreasing the depth so that in x=1.58 m, sediment concentration was 44 mg/l near the water surface that decreased about 57.48% in comparison to the bed sediment concentration. Average error percentage of the simulated results of sediment concentration in different basin sections in comparison to the experimental results indicates a better agreement with the experimental results in comparison to the numerical results by Shahrokhi et al. (2011). This shows the high capacity of Flow ED model in simulation of the sediment concentration in different sections of the pre-sedimentation basins.

References

Brooks H. N., (1963), Discussion of Boundary Shear Stresses in Curved Trapezoidal Channels. By A. T. Ippen and P. A. Drinker, ASCE Journal of Hydraulic Engineering, 89 (HY3).

Goula A. M., Thodoris M. K., Karapantsios D., and Zouboulis. A. I., (2007), A CFD Methodology for the Design of Sedimentation Tanks in Potable Water Treatment, Case Study: The Influence of a Feed Flow Control Baffle. Chemical engineering journal.

Imam E., Mc Corquodale J. A., (1983), Numerical Modeling of Sedimentation Tanks. Proc. ASCE 109.

Jayanti S., Narayanan S., (2004), Computational Study of Particle-Eddy Interaction in

Sedimentation Tanks. J. of environmental engineering, 130 (10), ASCE.

Larsen P., (1977), on the Hydraulics of Rectangular Settling Basins. Dept of Water Res. Engrg. Lind Institute of Technology, Lund, Sweden, 1001.

Liu B., Ma J., Huang S., Chen D., and Chen W., (2008), Two-Dimensional Numerical Simulation of Primary Settling Tanks by Hybrid Finite Analytic Method. Journal of Environmental Engineering, 134 (4), ASCE.

Liu B., Ma J., Luo L., Bai Y., Wang S. and Zhang J., (2010), Two-Dimensional LDV Measurement, Modeling and Optimal Design of Rectangular Primary Settling Tanks. J. Environmental Engineering, ASCE, 136(5): 501-507.

Lyn D. A., and Rodi W., (1990), Turbulence Measurement in Model Settling Tank. Journal of Hydraulic Engineering, 116 (1).

Mc. Corquodale J. A., Moursi A.M., El-Sebakhy I. S., (1988), Experimental Study of Flow in Settling Tanks. Journal of Environmental Engineering, 114 (5), ASCE.

Naser Gh., Karney B. W., and Salehi A. A., (2005), Two-Dimensional Simulation Model of Sediment Removal and Flow in Rectangular Sedimentation Basin. 10.1061 /ASCE.

Olsen N. B. R., (2009), A Three dimensional Numerical Model for Simulation of Sediment Movements in Water Intakes with Moltiblock Option. Department of Hydraulic and Environmental Engineering, the Norwegian University of Science and Technology. 177, pp.1

Rodi W., (1984), Turbulence Model and Their Application in Hydraulics, a State of the Art Review. Second edition, University of Karlsruhe, west Germany.

Shahrokhi, Rostami M., Azlin F., Syafalni. M. D., (2011), Numerical Modelling of the Effect of the Baffle Location on the Flow Field, Sediment Concentration and Efficiency of the Rectangular Primary Sedimentation Tanks. World Applied Sciences Journal, ISSN 1818-4952, 1296-1309.

Shahrokhi M., Rostami F. and Said Syafalni M. A. M., (2011), Computational Modelling of Baffle Configuration in the Primary Sedimentation Tanks. 2th ICEST, 392-396.

Shiba S. ASCE, A. M. Inoue. Y., (1975), Dynamic Response of Settling Basin. ASCE, Vol.101.

Stamou A. I., (2008), Improving the Hydraulic Efficiency of Water Process Tanks Using CFD Models. Chemical Engineering and Processing, Science Direct.

Tamayol A., Nazari M., Firoozabadi B., and Nabovati A., (2004), Effects of turbulent models and baffle position on hydrodynamics of settling tanks. Int. Mech. Eng. Con, Kuwait.

Ueberl J., Hager W. H., (1997), Improved Design of Final Settling Tanks. Journal of environmental engineering, March., ASCE, 123 (3).

Van Rijn L. C., (1987), Mathematical Modeling of Morphological Processes in the Case of Suspended Sediment Transport. Ph.D Thesis, Delft University of Technology.